

## Supporting Information

### Unexpectedly High Thermal Stability of Au Nanotriangles@mSiO<sub>2</sub> Yolk-Shell Nanoparticles

*Xiaobin Xie,<sup>\*†‡</sup> Wiebke Albrecht,<sup>†§</sup> Marijn A. van Huis,<sup>†</sup> and Alfons van Blaaderen<sup>\*†</sup>*

<sup>†</sup> Soft Condensed Matter, Debye Institute for Nanomaterials Science, Utrecht University, Princetonplein 5, 3584 CC Utrecht, the Netherlands

<sup>‡</sup> Present Address: Analytical & Testing Center, Sichuan University, Chengdu 610064, China

<sup>§</sup> Present Address: Department of Sustainable Energy Materials, AMOLF, Science Park 104, 1098 XG Amsterdam, The Netherlands.

1. Chemicals
2. Synthesis
  - 2.1 Synthesis and purification of Au NTs
  - 2.2 Synthesis of Au NT@mSiO<sub>2</sub> core shell nanoparticles
  - 2.3 Synthesis of Au NT@mSiO<sub>2</sub> yolk shell nanoparticles
3. Liquid-cell experiments
4. Heating experiments
5. Characterization
6. FDTD simulations
7. Key physical parameters of Au
8. Supporting Figures
9. Supporting Movie Information

Movie S1

Movie S2

## 1 Chemicals

Used chemicals were hydrogen tetrachloroaurate (III) hydrate ( $\text{HAuCl}_4$ , 99.9%, Sigma), sodium borohydride ( $\text{NaBH}_4$ , 96%, Sigma), L-ascorbic acid (AA, 99.98%, Sigma), sodium hydroxide ( $\text{NaOH}$ , 98%, Sigma), tetraethyl orthosilicate (TEOS,  $\text{Si}(\text{OC}_2\text{H}_5)_4$ , 99.0%, Sigma-Aldrich), methanol ( $\text{MeOH}$ , 99%, Sigma), and cetyltrimethyl-ammonium chloride (CTAC,  $\geq 99\%$ , Sigma), and CTAC solution (25wt% in water, Sigma-Aldrich). All chemicals were used as received without further purification. Also, de-ionized water with a resistivity of  $18.2 \text{ M}\Omega\cdot\text{cm}$  at  $25^\circ\text{C}$  was used in the experiments.

## 2 Synthesis

### 2.1 Synthesis and purification of Au NTs

The Au NTs were synthesized by a modification of a previously reported synthesis.<sup>1</sup> (1) Au seeds@CTAC: 25  $\mu\text{L}$  of 50 mM  $\text{HAuCl}_4$  was mixed with 4.70 mL of 0.10 M CTAC solution in a 20 mL glass vial. Next, 300  $\mu\text{L}$  of fresh prepared 10 mM  $\text{NaBH}_4$  was injected into the above mixture while stirring. The seeds solution was strongly stirred for 2 min. After that, it was kept at room temperature for at least 2 hours. After 2 hours, the Au seeds solution was diluted 10 times by mixing 0.50 mL of Au seeds and 4.50 mL of 0.10 M CTAC. (2) 1.60 mL of 0.10 M CTAC, 40  $\mu\text{L}$  of 50 mM  $\text{HAuCl}_4$ , and 30  $\mu\text{L}$  of 10 mM KI were added into 8.00 mL of de-ionized water in a 20 mL glass vial one by one. This solution was marked as solution-A. (3) 60 mL of deionized water was added into a 250 mL round-bottom flask. 60 mL of 0.10 M CTAC and 900  $\mu\text{L}$  of 10 mM KI were injected into the deionized water. This solution was marked as solution-B. (4) 40  $\mu\text{L}$  and 1.20 mL of 0.10 M AA solution were injected into solution-A and solution-B, respectively, while stirring. After both the solution-A and solution-B turned colorless in 30 seconds, 100  $\mu\text{L}$  of diluted Au seeds was injected into solution-A. Stirring continued for about one minute. All solution-A was added into solution-B while stirring. After the two solutions were well mixed, it was left undisturbed for about 2 hours, which allowed growth of the Au nanocrystals. (5) Purification: After allowing growth for about 2 hours, 34.0 mL of solution-B and 4.50 mL of 25 wt% CTAC were mixed in a 50 mL centrifuge tube, and then left undisturbed for 12 hours. The suspension was removed carefully, and the sediment was suspended in 35.0 mL of 0.01 M CATC and served as a stock solution for further use.

### 2.2 Synthesis of Au NT@mSiO<sub>2</sub> core shell nanoparticles

The Au NT@mSiO<sub>2</sub> core shell (CS) nanoparticles (NPs) were synthesized based on our previous work.<sup>2</sup> In brief, a volume of 10 mL of Au NTs stock solution ( $\lambda_{\text{LSPR}} = 657 \text{ nm}$ , extinction = 2.1) was centrifuged at 9000 rpm for 10 minutes (Rotina 380R Hettich centrifuge). After centrifuging, the suspension was removed and the sediment was suspended in 10 mL of deionized water and transferred into a 20 mL glass vial. 500  $\mu\text{L}$  of 0.1 M CATC and 100  $\mu\text{L}$  of 0.10 M NaOH were added into above Au NTs solution. Lastly, 200  $\mu\text{L}$  of 20 vol% (10 vol% for 10 nm mSiO<sub>2</sub> shell) TEOS in methanol was injected into the above solution in one shot under stirring. The solution was stirred for 45-48 hours.

### 2.3 Synthesis of Au NT@mSiO<sub>2</sub> yolk shell nanoparticles

The Au NT@mSiO<sub>2</sub> yolk shell (YS) nanoparticles (NPs) were synthesized based on our previous report.<sup>2</sup> In brief, a volume of 10 mL (6 mL for 20 nm mSiO<sub>2</sub> shell) of Au NTs storage solution was centrifuged at 9000 rpm (Rotina 380R Hettich centrifuge) for 10 minutes. After centrifuging, the suspension was removed and the sediment was suspended in 10 mL of deionized water and transferred into a 20 mL glass vial. 150  $\mu\text{L}$  of 0.1 M CATC and 100  $\mu\text{L}$  of 0.10 M NaOH were added into above Au NTs solution. Lastly, 200  $\mu\text{L}$  of 20 vol% TEOS in methanol was injected into the above solution in one shot under stirring. The solution was stirred for 45-48 hours.

## 3 Liquid-cell experiments

**Sample preparation:** The 10 mL of as-prepared Au NT@mSiO<sub>2</sub> yolk-shell NPs were centrifuged at 9000 rpm for 10 minutes. After centrifuging, the suspension was carefully removed and washed by deionized water twice. Finally, the sediment was suspended in 2 mL of deionized water for further use.

**Assembly of LC-TEM chips:** (1) The LC-TEM chips were pretreated using 20 seconds of Ar/O<sub>2</sub> (20 v% of O<sub>2</sub>) plasma treatment. (2) The bottom chip (Hummingbird Scientific, SQ Spacer 250 nm Parallel (50 nm, 50  $\mu\text{m}$ , 200  $\mu\text{m}$ )) was put on a LC-TEM holder (Hummingbird Scientific) and 2  $\mu\text{L}$  of above Au NT@mSiO<sub>2</sub> yolk-shell NPs was dropped on a liquid-cell bottom chip. (3) A top chip (Hummingbird Scientific, SQ Window (50 nm, 50  $\mu\text{m}$ , 200  $\mu\text{m}$ )) was carefully put onto the bottom chip and the chips were sealed.

**Recording TEM images and videos:** The experiments were performed on a FEI Tecnai F20 TEM and a FEI Talos F200X, both operating at 200 kV. The videos were recorded by TIA software (Version 5.0) using preview mode and a recording speed of 2 fps. The final videos shown in Supporting Information were processed by ImageJ software (Version 1.51j8) and are displayed 3 times faster than real time.

#### 4 Heating experiments

**In-situ heating:** In-situ heating (S)TEM experiments were performed using a heating holder made by DENS Solutions. Heating chips with electron beam transparent SiN windows were provided by the same company. (1) The heating chips were pretreated using Ar/O<sub>2</sub> (20 vol.% of O<sub>2</sub>) plasma treatment for 20 seconds. (2) 8 μL of as-prepared Au NTs or Au NT@mSiO<sub>2</sub> NPs were dropped on a heating chip and dried in ambient air at room temperature (RT). (3) The heating chip with sample was mounted on a heating holder (DENS-H-SH30-FS01). (4) The heating holder was inserted into the Electron Microscope used, which was a FEI Talos F200X. (5) Normally, the heating procedure started from 20 °C to an aim temperature with a step temperature of 100 °C, about 5 min waiting at each temperature before acquired images. The heating curve for each sample is presented in the supporting figures.

**Ex-situ heating (oven heating in air):** (1) 10 mL of as-prepared Au NT@mSiO<sub>2</sub> core-shell and/or NPs was centrifuged at 9000 rpm for 10 minutes. After centrifugation, the suspension was removed and the sediment was suspended in 500 μL of deionized water. (2) 100 μL of above solution was dropped into a 4 mL sample bottle and drying naturally at RT. (3) The oven was set and stabilized at the annealing temperatures of 200, 300, 400, 500, and 600 °C, respectively. (4) The bottle with drying samples was put into the oven (Carbolite, Laboratory Chamber Furnace-ELF) which is at a specific temperature and kept undisturbed for one hour. (5) removing the bottle from the oven and cooling down naturally in atmosphere. (6) After cooling down to RT, the samples were re-dissolved into 1 ml of de-ion water. (7) Measuring the UV-VIS spectra of each sample after heating.

**Ex-situ heating (furnace heating in N<sub>2</sub>):** (1) The sample preparation was following the same protocol described above. (2) The tube furnace (Carbolite, Wire Wound Tube Furnace – TZF 12) was set to the desired annealing temperatures of 200 °C, 300 °C, 400 °C, 500 °C, and 600 °C, respectively. (3) The temperature was increased by raising the temperature with a rate of 5 °C/min, keeping the oven at the annealing temperature for 60 min, and then cooling down naturally to RT. (4) N<sub>2</sub> gas was flowed for at least one hour before starting the heating program and N<sub>2</sub> gas flowed continuously until the temperature was back to RT. (5) After cooling down to RT, the samples were re-dissolved into 1 ml of de-ion water. (6) Measuring the UV-VIS spectra of each sample after heating.

## 5 Characterization

Ultraviolet-Visible (UV-Vis) spectroscopy was performed with a Lambda 750 UV-Vis spectrograph (Perkin Elmer). Transmission electron microscopy (TEM) images and high angular annular dark field scanning transmission electron microscopy (HAADF-STEM) images were acquired with a FEI Talos F200X, operated at 200 kV. The particle sizes of the Au NTs and deformed Au NTs were measured from TEM or STEM images, whereby 100-200 particles were measured for each sample. The results were denoted by  $\mu \pm \sigma$ , where  $\mu$  is the mean size and  $\sigma$  is the standard deviation.

## 6 FDTD Simulations

The FDTD simulations were carried out using FDTD Solutions software version 8.19 developed by Lumerical Solutions. A total field scattered field source with a wavelength range of 300 nm to 900 nm was used to simulate the interaction between a propagating plane wave and the nanoparticles. The nanoparticle was surrounded by a virtual boundary with a proper size. A three-dimensional non-uniform mesh was used with a fine mesh grid size of 0.05 nm for calculating the extinction spectra of the nanoparticles. The refractive index of the surrounding medium was set to that of water (1.33). The Au NT model was built as a triangular prism with an edge length of 66 nm and a thickness of 22 nm. The dielectric functions of metals were acquired by fitting the points from the data of Johnson and Christy.<sup>3</sup>

## 7 Key physical parameters of Au

A number of physical parameters of bulk Au is summarized in Table S1, which include its face-centered-cubic FCC lattice parameters, bond dissociation energy of same metal atoms (M-M), surface energy, and the standard reduction potentials.<sup>4-7</sup>

**Table S1.** Key physical parameters of Au

	<b>Au</b>
<b>Lattice Parameters (Å)</b>	4.078
<b>Atomic Radius (Å)</b>	1.442
<b>Bond Dissociation Energy (Au-Au, kJ / mol)</b>	226
<b>Density of bulk Au (g/cm<sup>3</sup>)</b>	19.30
<b>Surface Energy of Au (111) (J/m<sup>2</sup>)</b>	0.71

<b>Surface Energy of Au (100) (J/m<sup>2</sup>)</b>	0.86
<b>Weighted Surface Energy of Au (J/m<sup>2</sup>)</b>	0.75

The key parameters of Au NTs and the Au nanosphere (NS) with same volume of Au NT were calculated and listed in Table S2.

**Table S2.** Key parameters of Au NT and Au NS

<b>Shape</b>	<b>Au NT</b>	<b>Au NS</b>
<b>Edge Length / Radius (nm)</b>	66	20.18
<b>Volume (nm<sup>3</sup>)</b>	3.4×10 <sup>4</sup> (34409)	3.4×10 <sup>4</sup> (34405)
<b>Surface Area(nm<sup>2</sup>)</b>	6.3×10 <sup>3</sup> (6266)	5.1×10 <sup>3</sup> (5114)
<b>Surface Area to Volume Ratio (nm<sup>2</sup> / nm<sup>3</sup>)</b>	0.18 (0.1821)	0.15 (0.1486)
<b>Specific Surface Area (m<sup>2</sup>/g)</b>	9.3	7.8

## 8 Supporting Figures

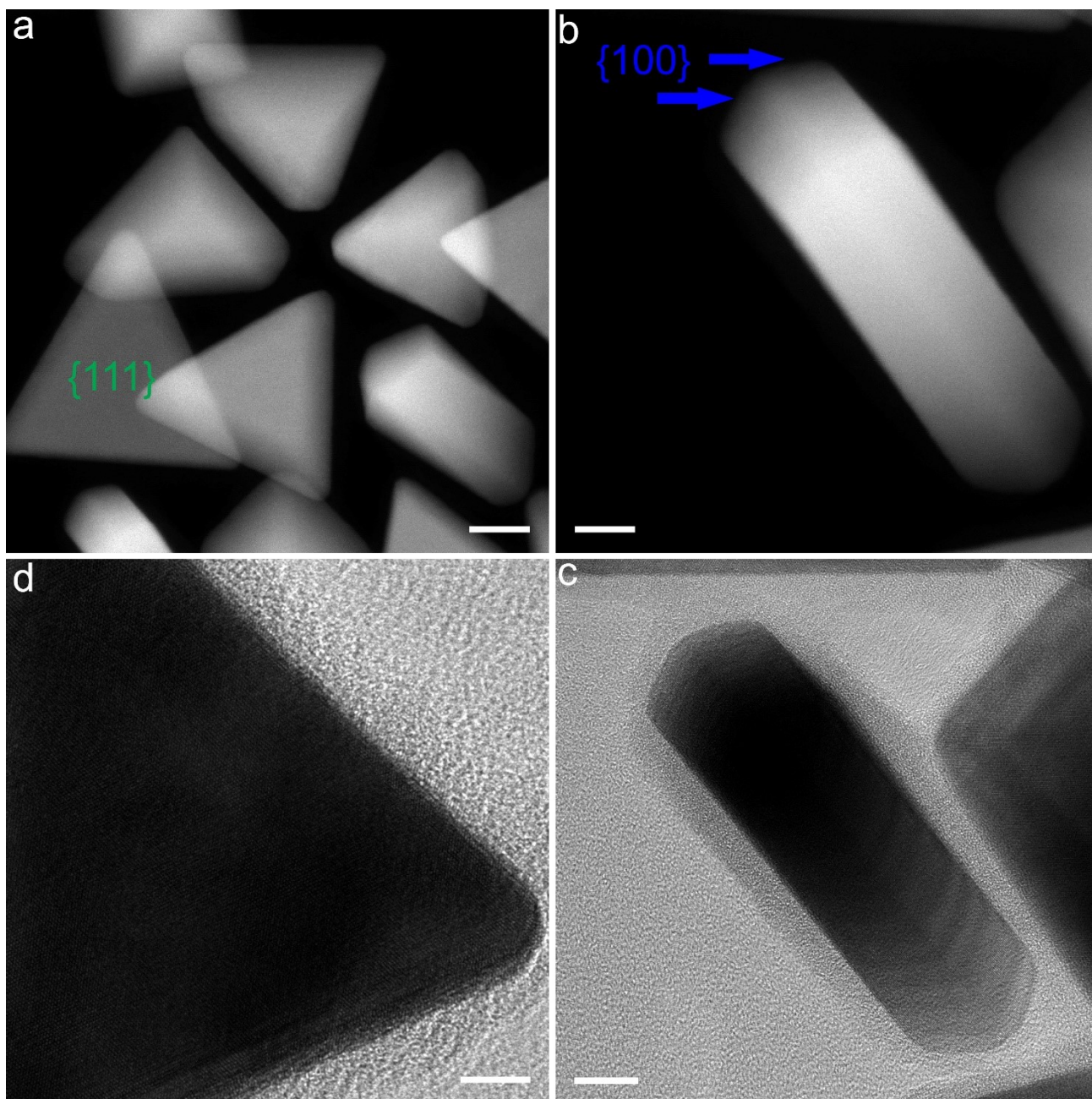


**Figure S1.** Au NTs viewed at different angles. HAADF-STEM images of Au NTs (a & b). HRTEM images of Au NT (c & d). The scale bars indicate: a) 100 nm, b) 10 nm, c) 10 nm, and d) 5 nm.

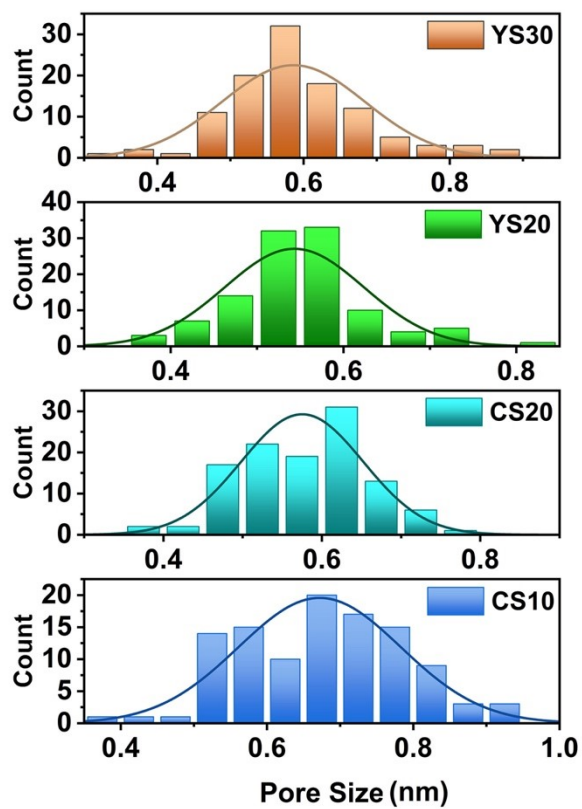


**Figure S2.** Pore size distribution of mSiO<sub>2</sub> shell of Au NT@mSiO<sub>2</sub> CS and YS particles.



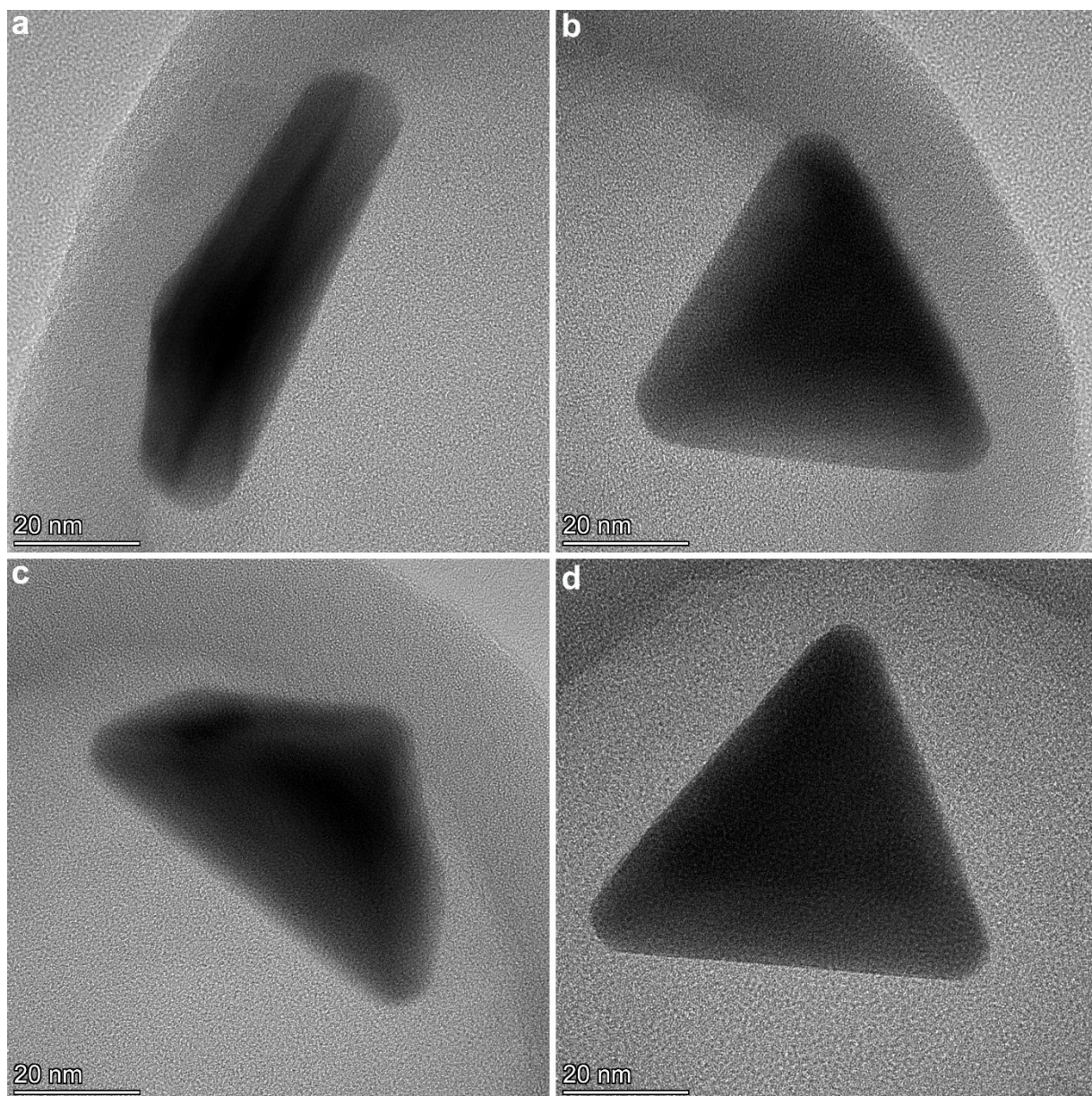


**Figure S3.** HRTEM images of Au NT@mSiO<sub>2</sub> YS-20.



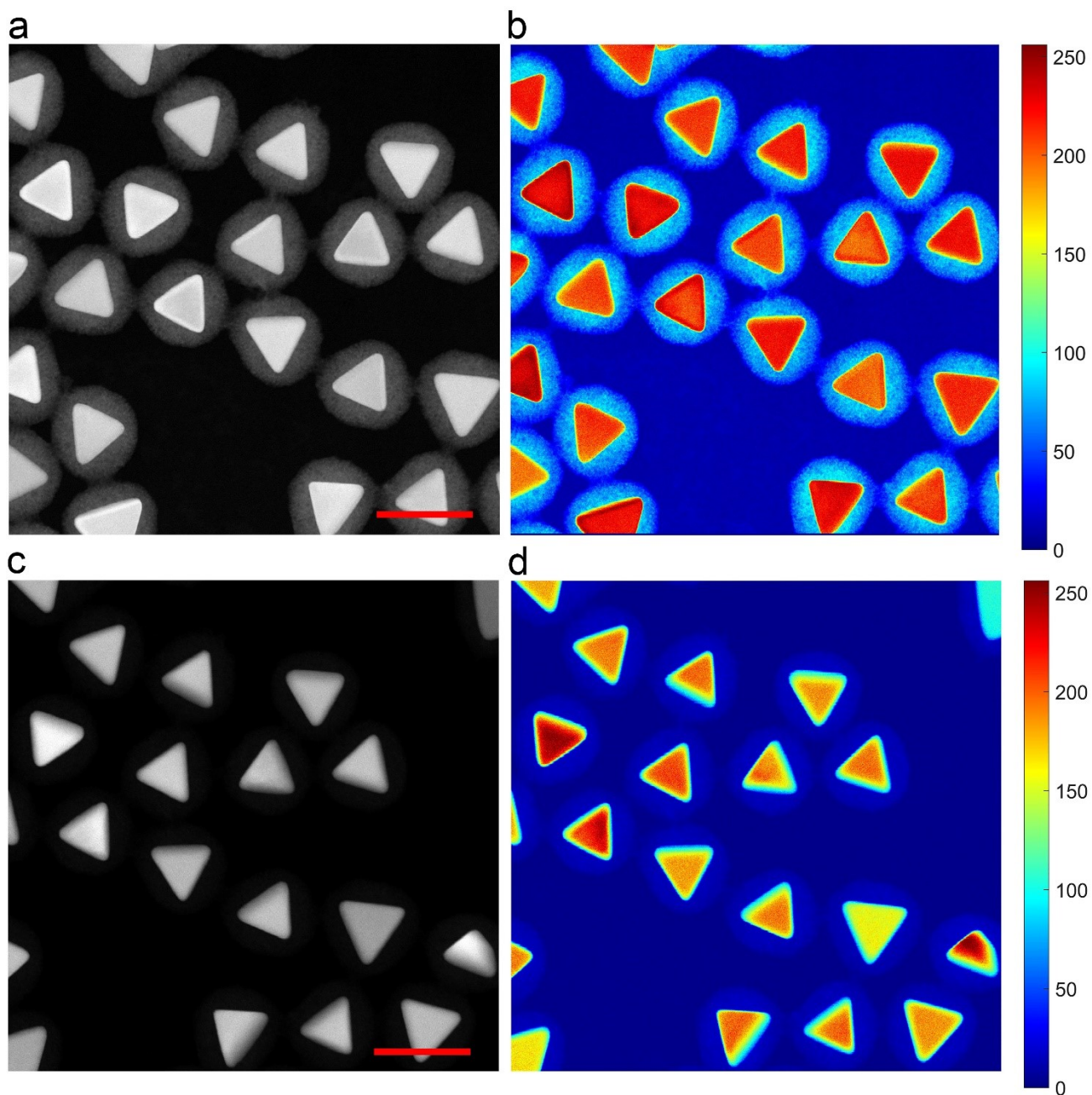


**Figure S4.** HAADF-STEM images of Au NT@mSiO<sub>2</sub> acquired with different camera lengths. The camera length used for a) is 206 mm, and for c) is 98 mm. b) and d) are color maps of a) and c), respectively. The scale bar indicates 100 nm.

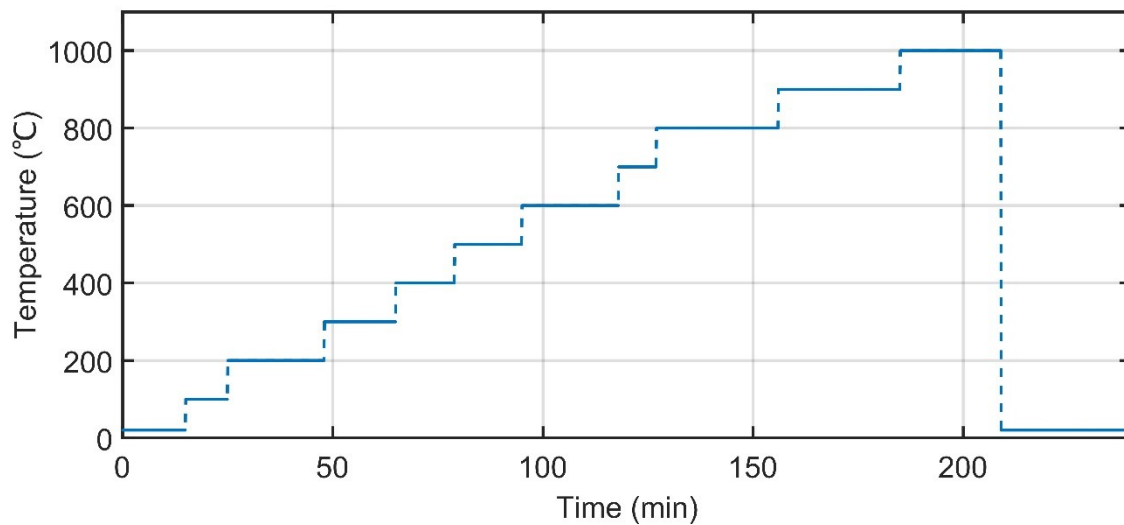


**Figure S5.** In-situ heating curve for Au NTs.

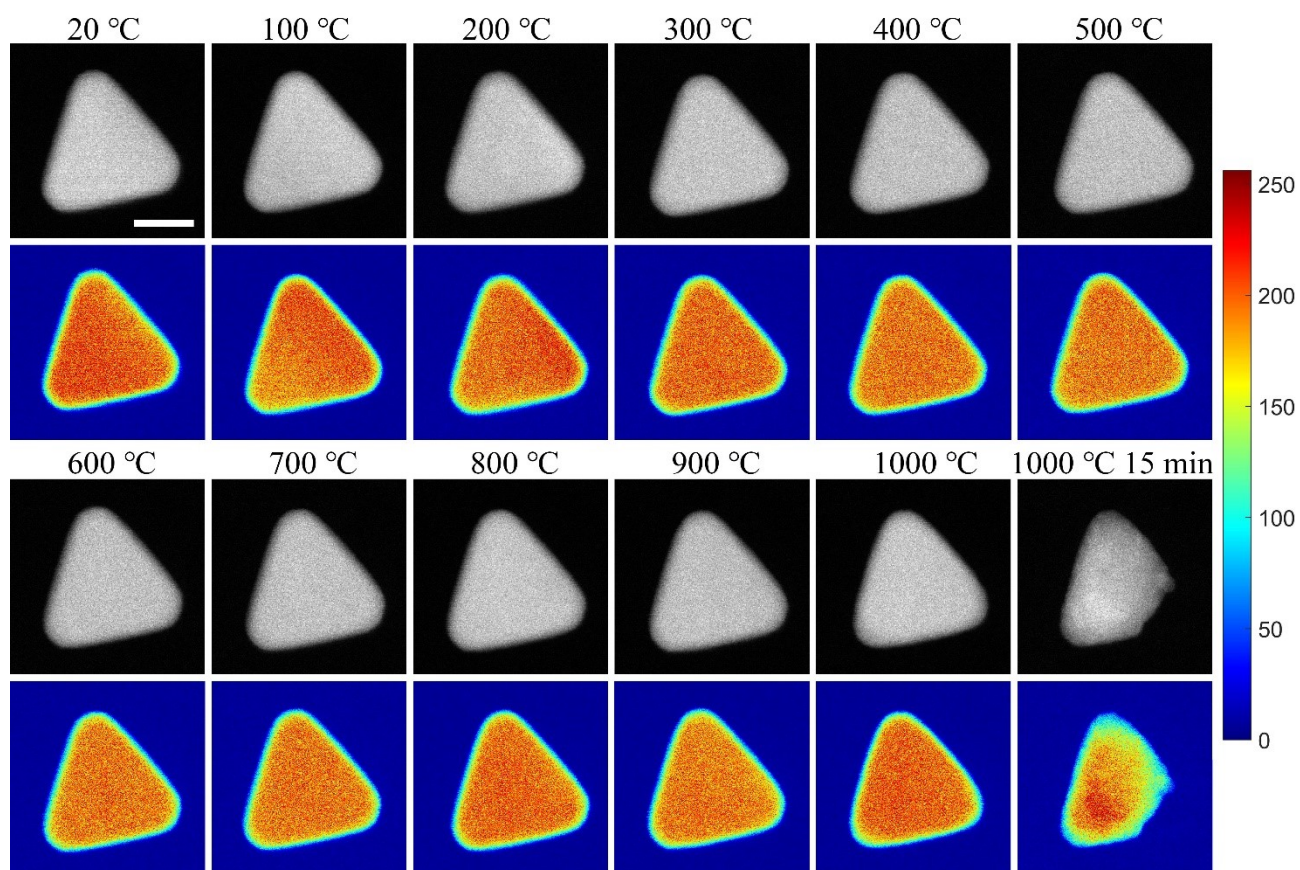


**Figure S6.** HAADF-STEM images of a single Au NT acquired at different heating temperature in an in-situ heating S/TEM experiment. The scale bar indicates 50 nm.

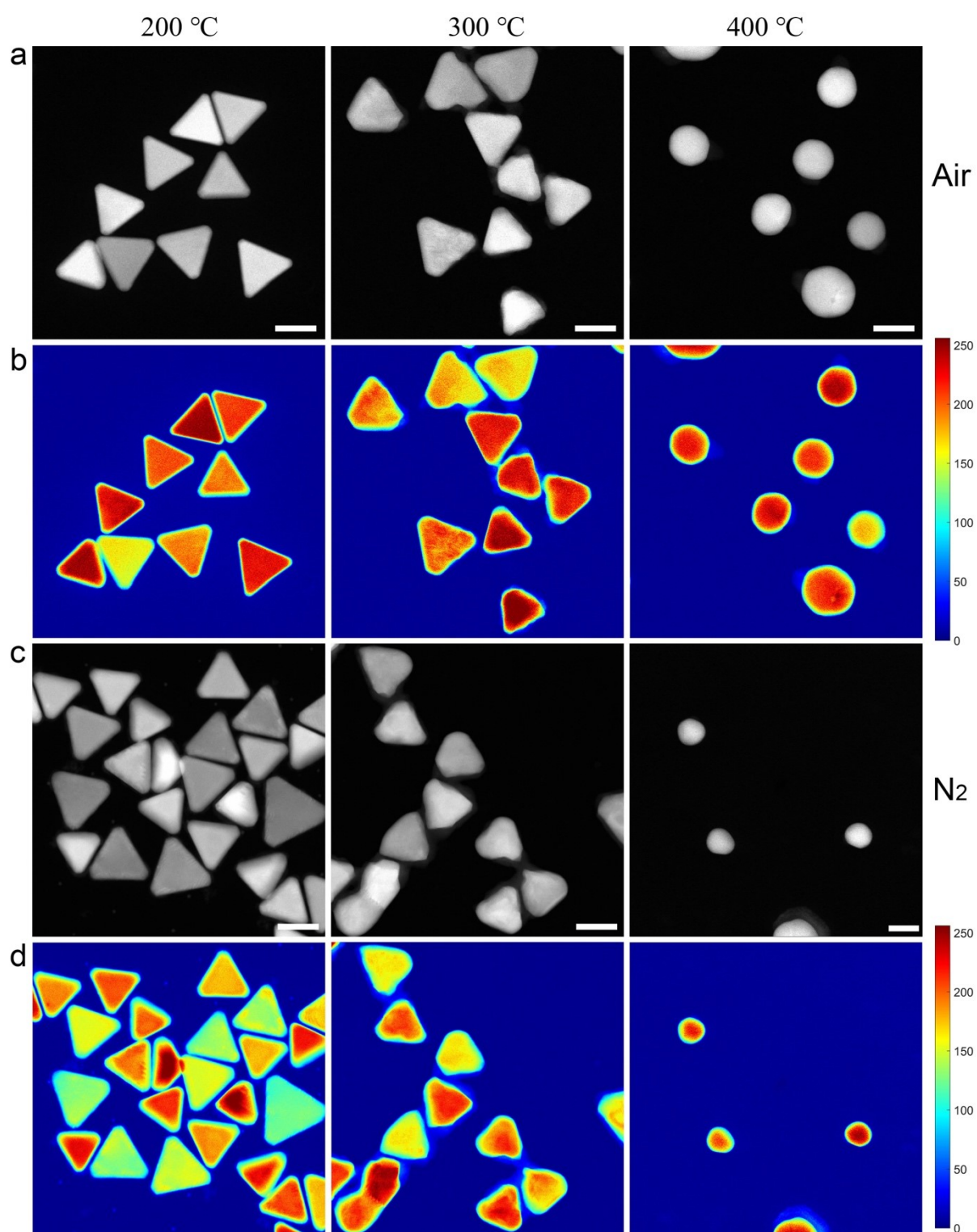


**Figure S7.** Oven heating of Au NTs on SiO film at 200, 300, and 400 °C for one hour in air or N<sub>2</sub>. a & b) HAADF-STEM images of Au NTs after oven heating in air; c & d) HAADF-STEM images of Au NTs after oven heating in N<sub>2</sub>. The scale bar indicates 50 nm.



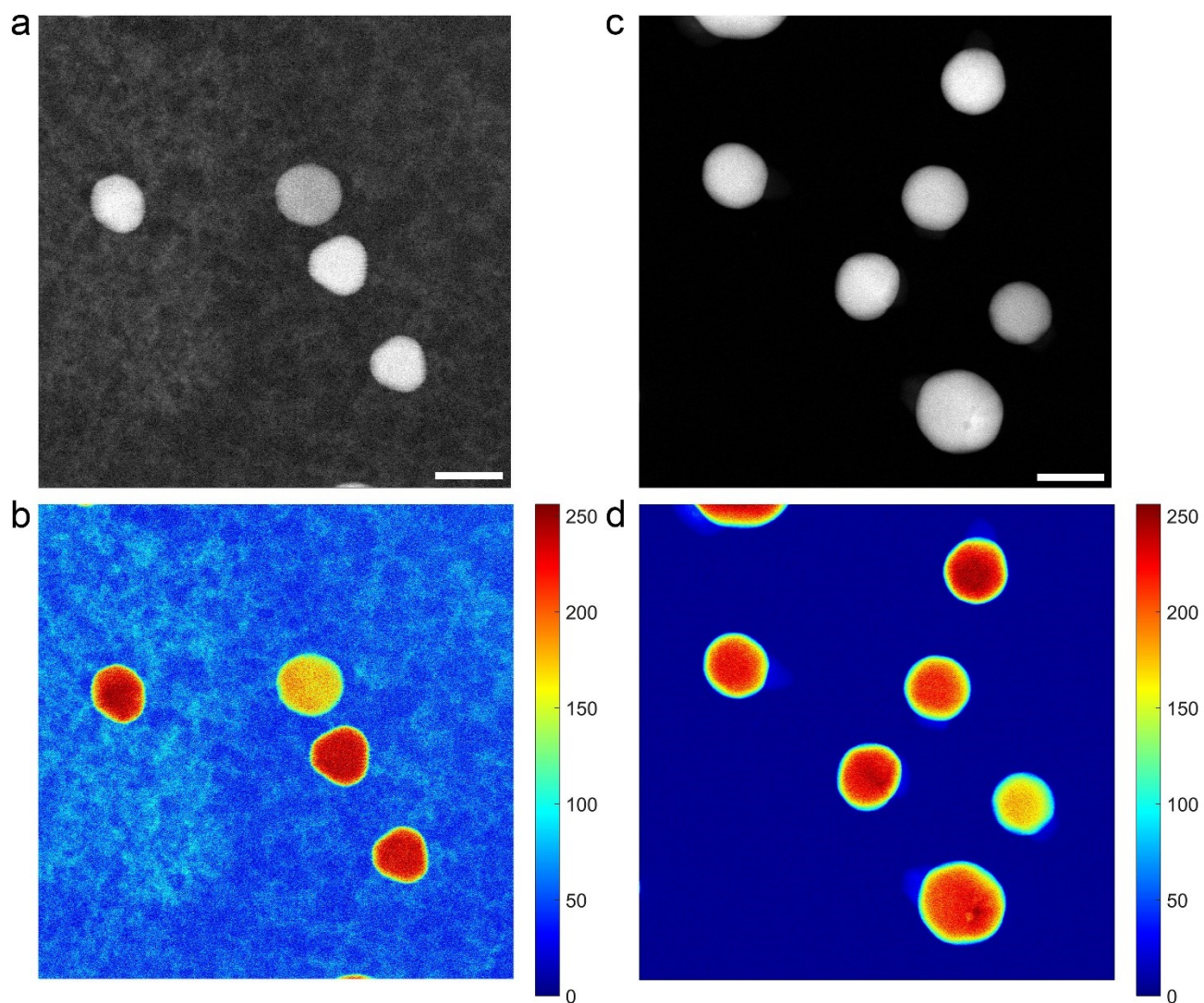


**Figure S8.** Oven heating of Au NTs on different substrates at 400 °C for one hour in air. a & b) on a TEM grid with SiO film; c & d) on a heating chip with SiN membrane. The scale bar indicates 50 nm.

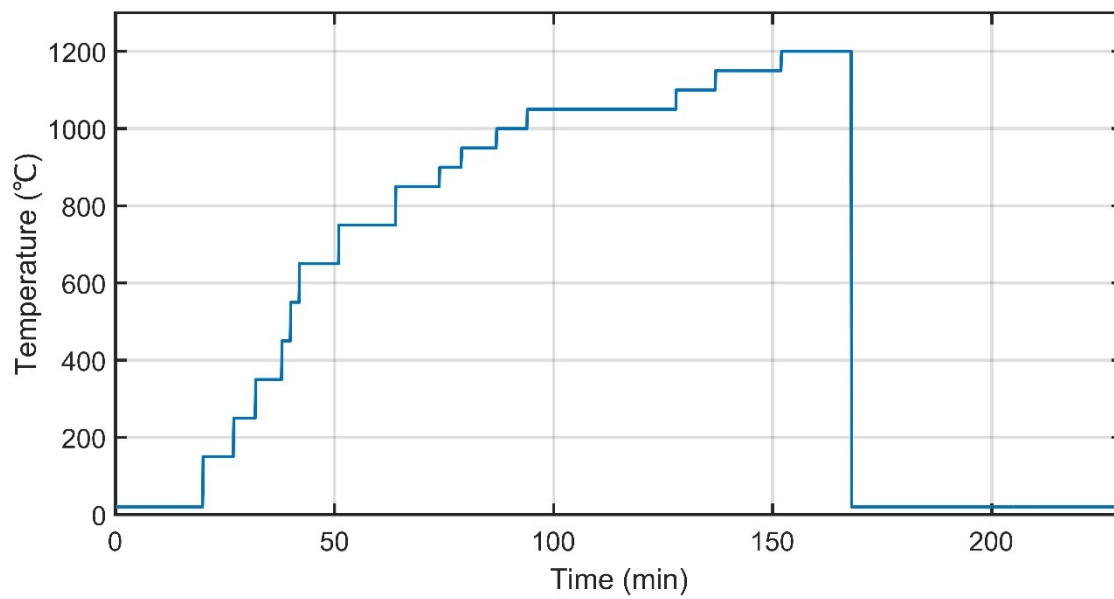


**Figure S9.** In-situ heating curve for Au NT@mSiO<sub>2</sub> CS NPs.

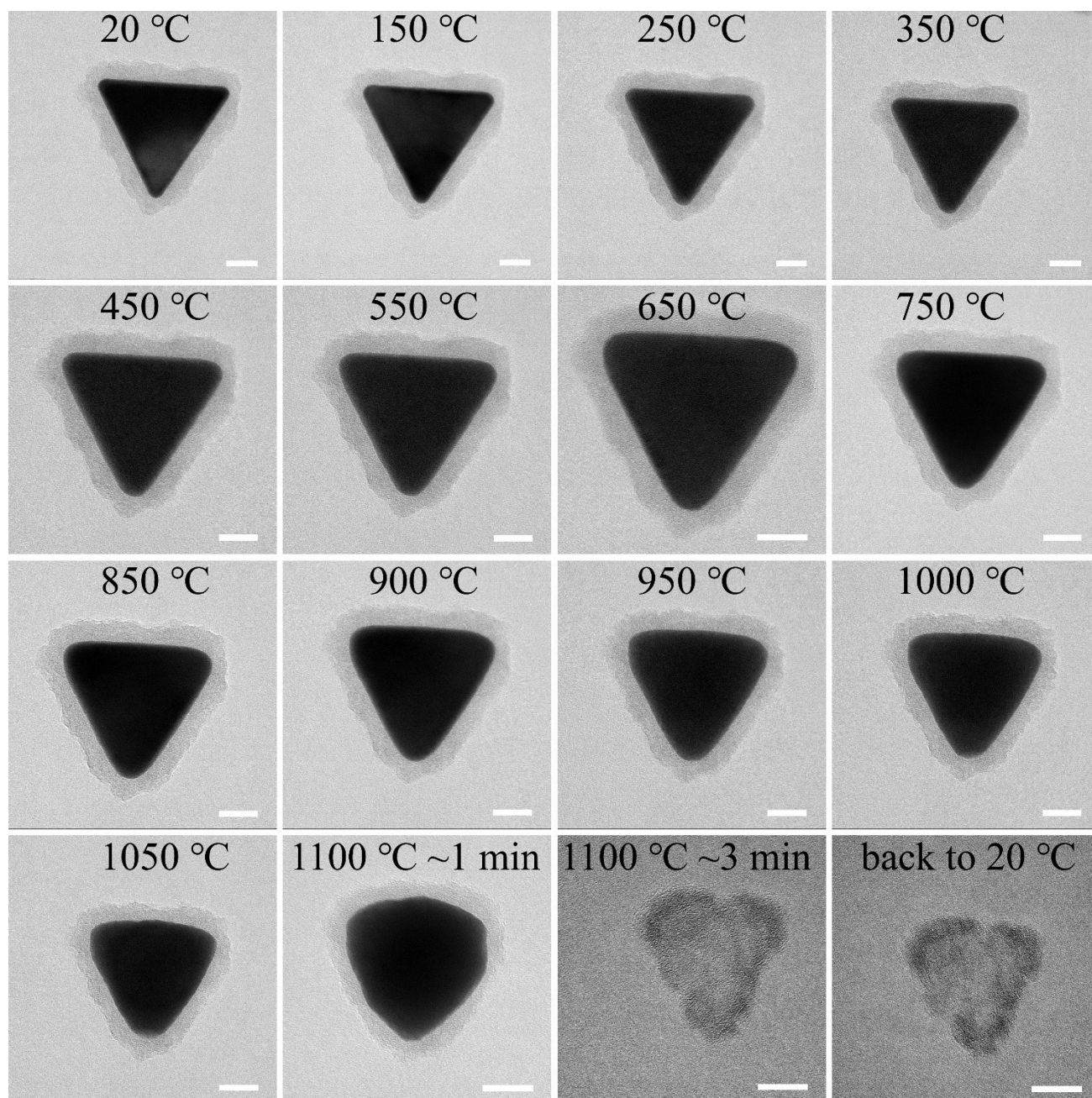


**Figure S10.** Shape evolution of Au NT@mSiO<sub>2</sub> CS NPs. TEM images of a single Au NT@mSiO<sub>2</sub> CS NPs acquired at different heating temperature in an in-situ heating experiment. Scale bars indicate 20 nm for all in all TEM images.



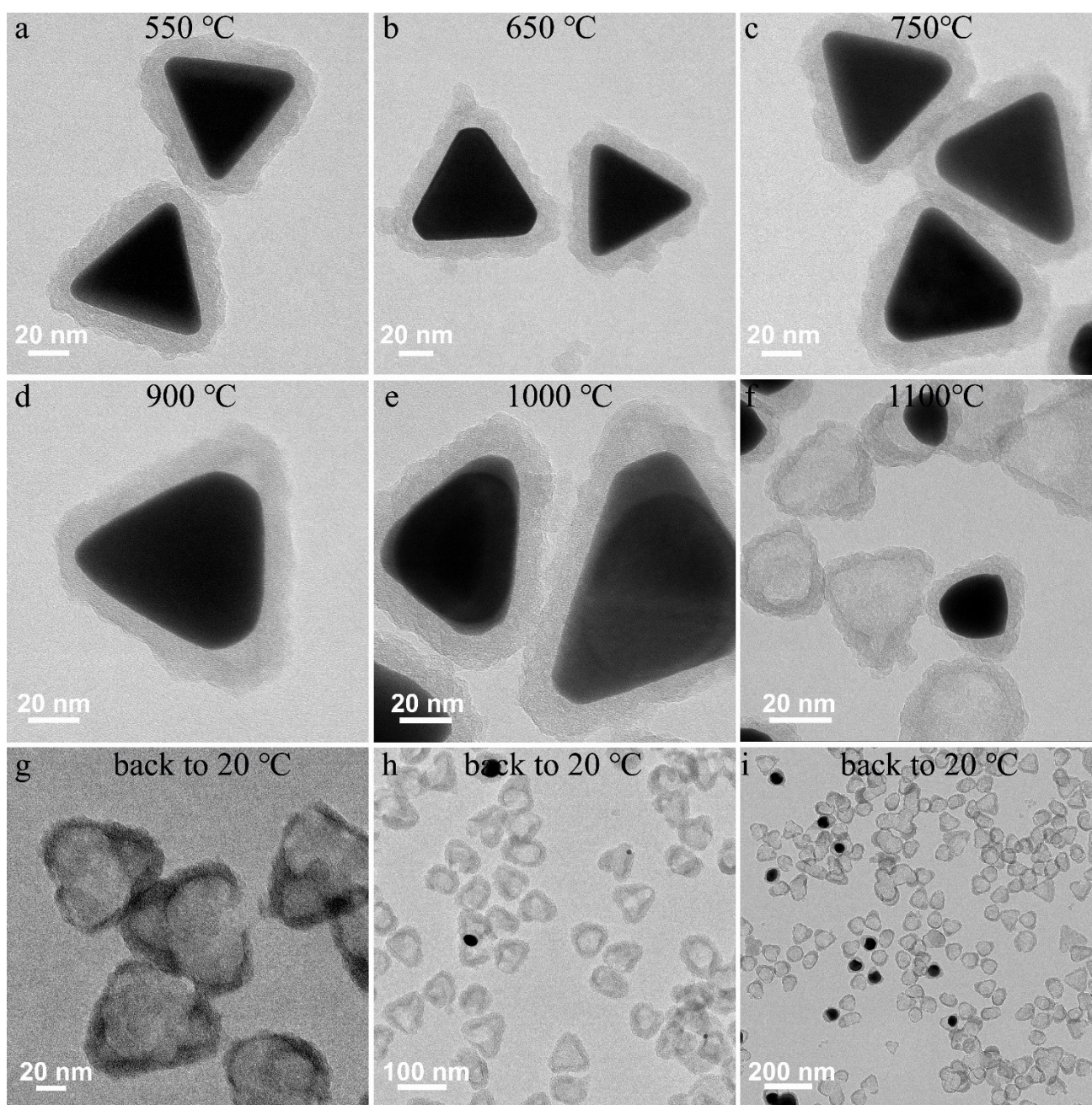


**Figure S11.** Shape evolution of Au NT@mSiO<sub>2</sub> CS NPs. TEM images of Au NT@mSiO<sub>2</sub> CS NPs acquired at different heating temperature at different windows (unexposed to electron beam before imaging) in an in-situ heating experiment.



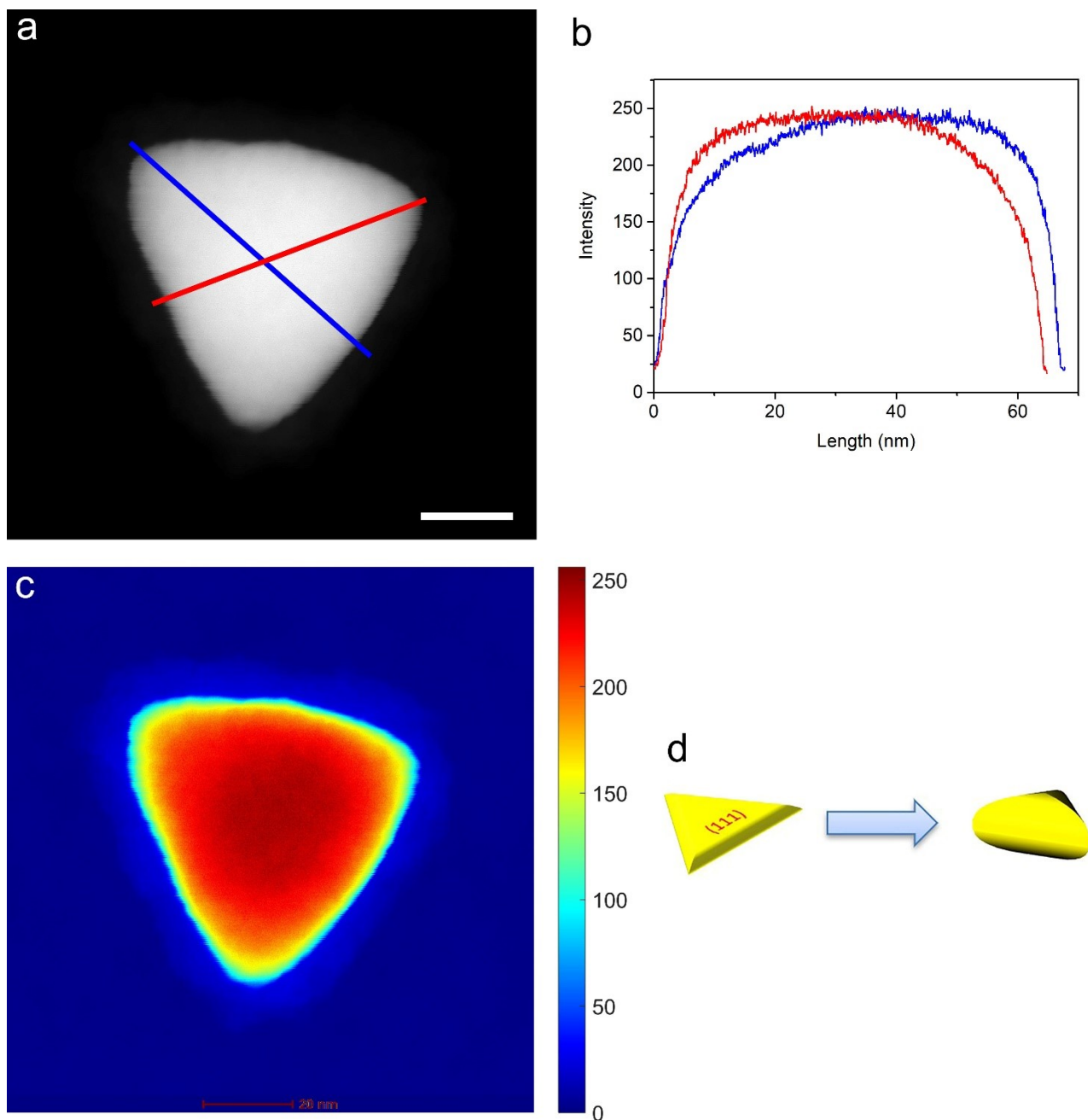


**Figure S12.** Morphology of Au NT@mSiO<sub>2</sub> at 1050 °C. a) STEM image of a single Au NT@mSiO<sub>2</sub> CS NPs acquired at 1050 °C, the scale bar indicates 20 nm; b) profiles of the contrast of STEM image from a; c) color map of STEM image in a); and d) scheme shows the deformation of Au NT.

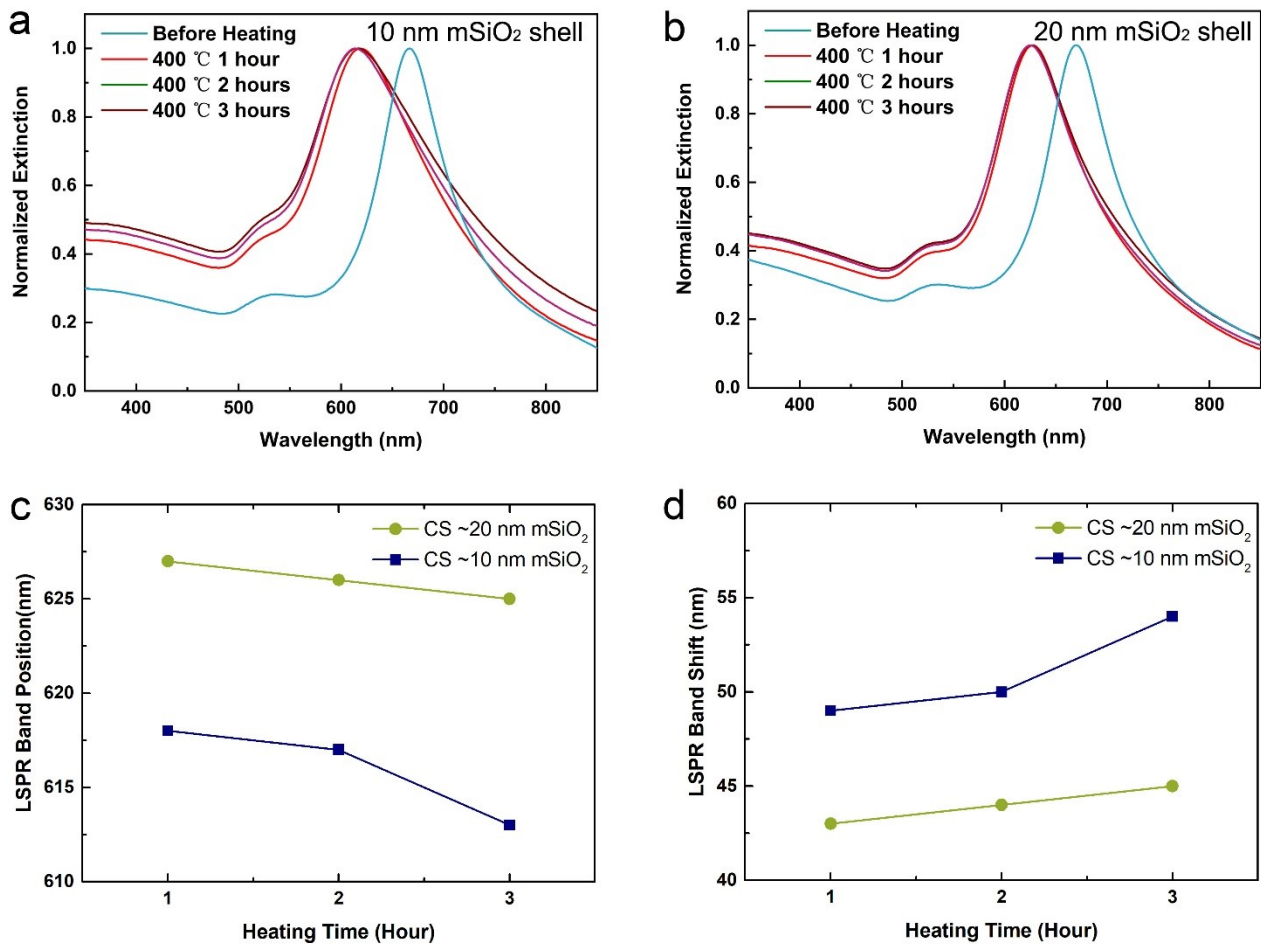


**Figure S13.** UV-VIS spectra of Au NT@mSiO<sub>2</sub> CS-10 (a), Au NT@mSiO<sub>2</sub> CS-20 (b) heated in oven in air for one to three hours, and c) LSPR band positions, d) LSPR band shifts.

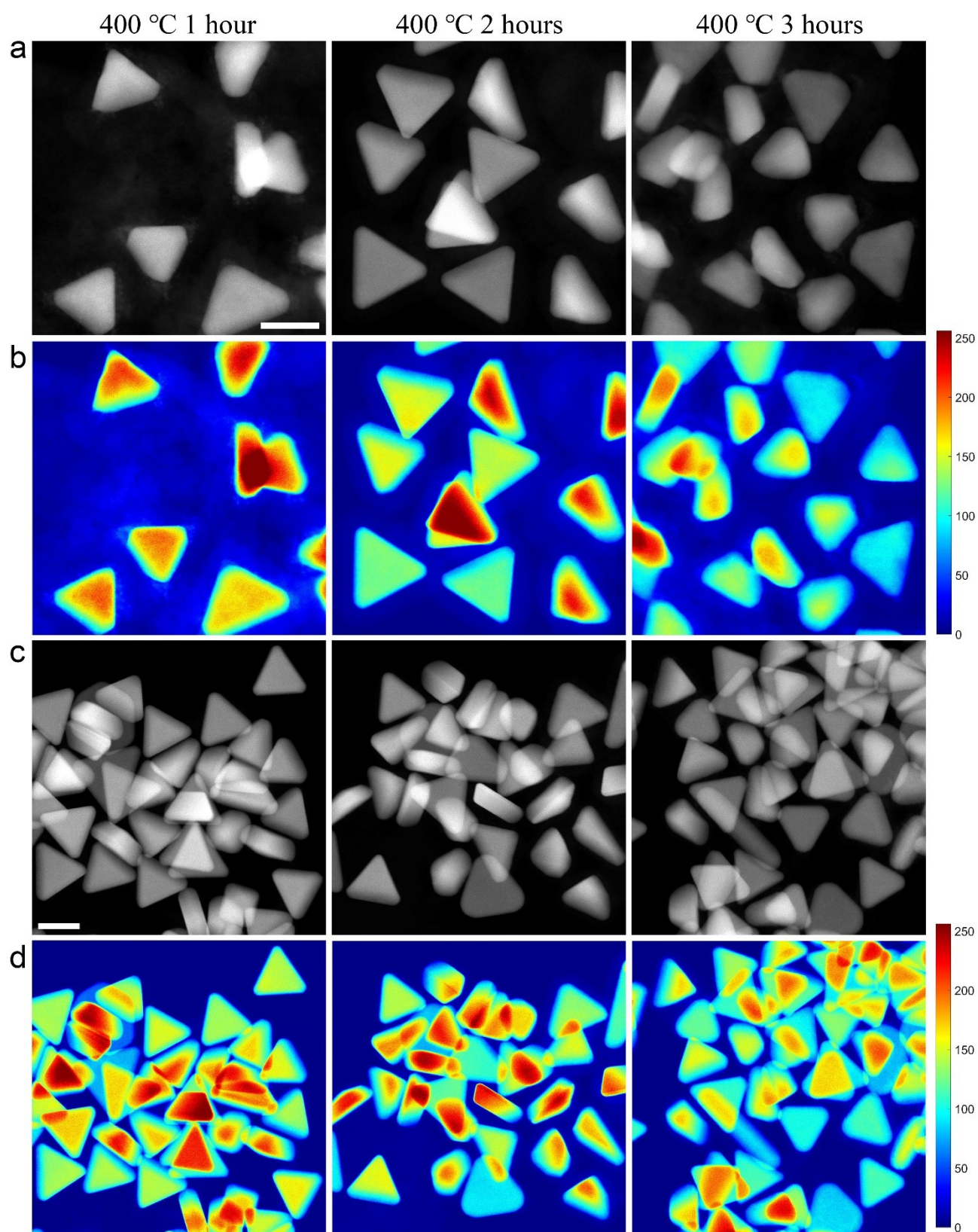


**Figure S14.** HAADF-STEM images of Au NT@mSiO<sub>2</sub> CS NPs heated in oven in air for one to three hours at 400 °C. a) Au NT@mSiO<sub>2</sub> CS-10, c) Au NT@mSiO<sub>2</sub> CS-20; b) and d) are color maps of a) and c), respectively. The scale bar indicates 50 nm.



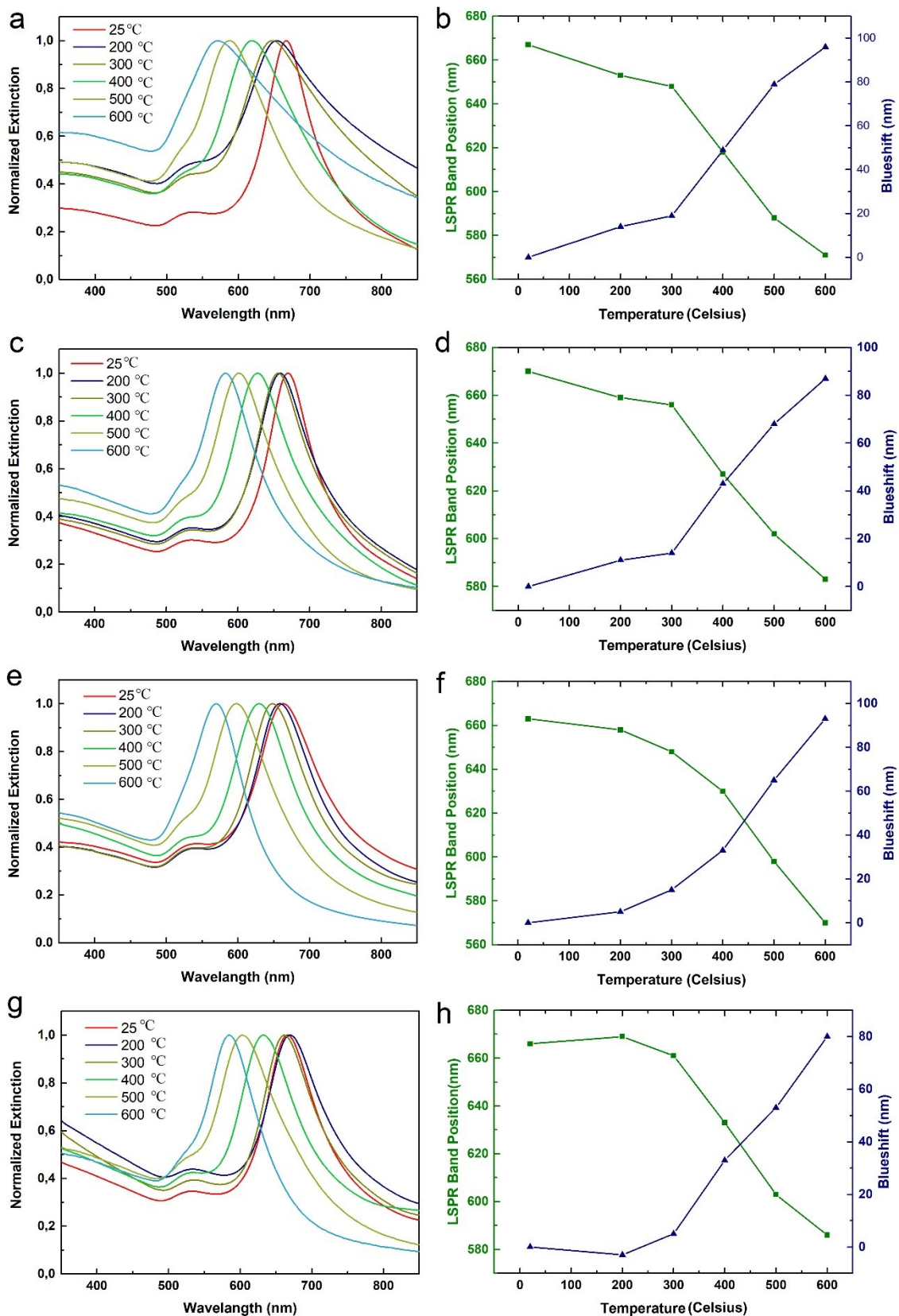


**Figure S15.** UV-VIS spectra of Au NT@mSi<sub>2</sub> CS-10 (a & b), Au NT@mSi<sub>2</sub> CS-20 (c & d), Au NT@mSi<sub>2</sub> YS-20 (e & f) and Au NT@mSi<sub>2</sub> YS-30 (g & h) before and after heating in oven in air.

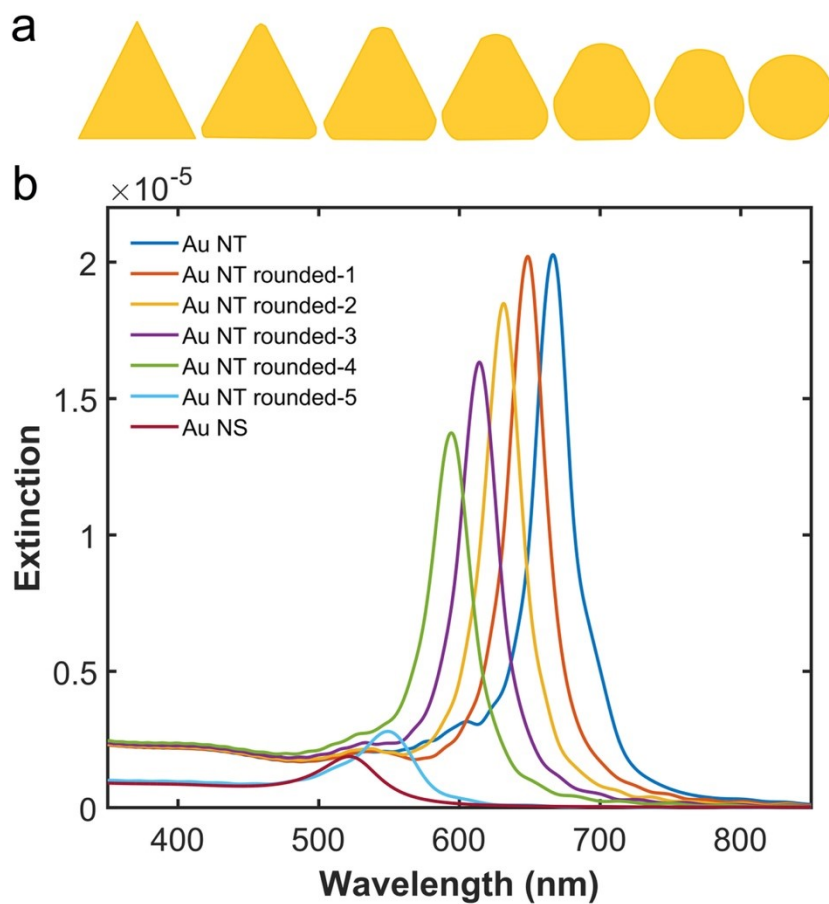


**Figure S16.** FDTD simulations of Au NT, rounded Au NT and Au NS. a) scheme shows the simulated models Au NT, rounded Au NT, and Au NS, b) FDTD simulated spectrum.

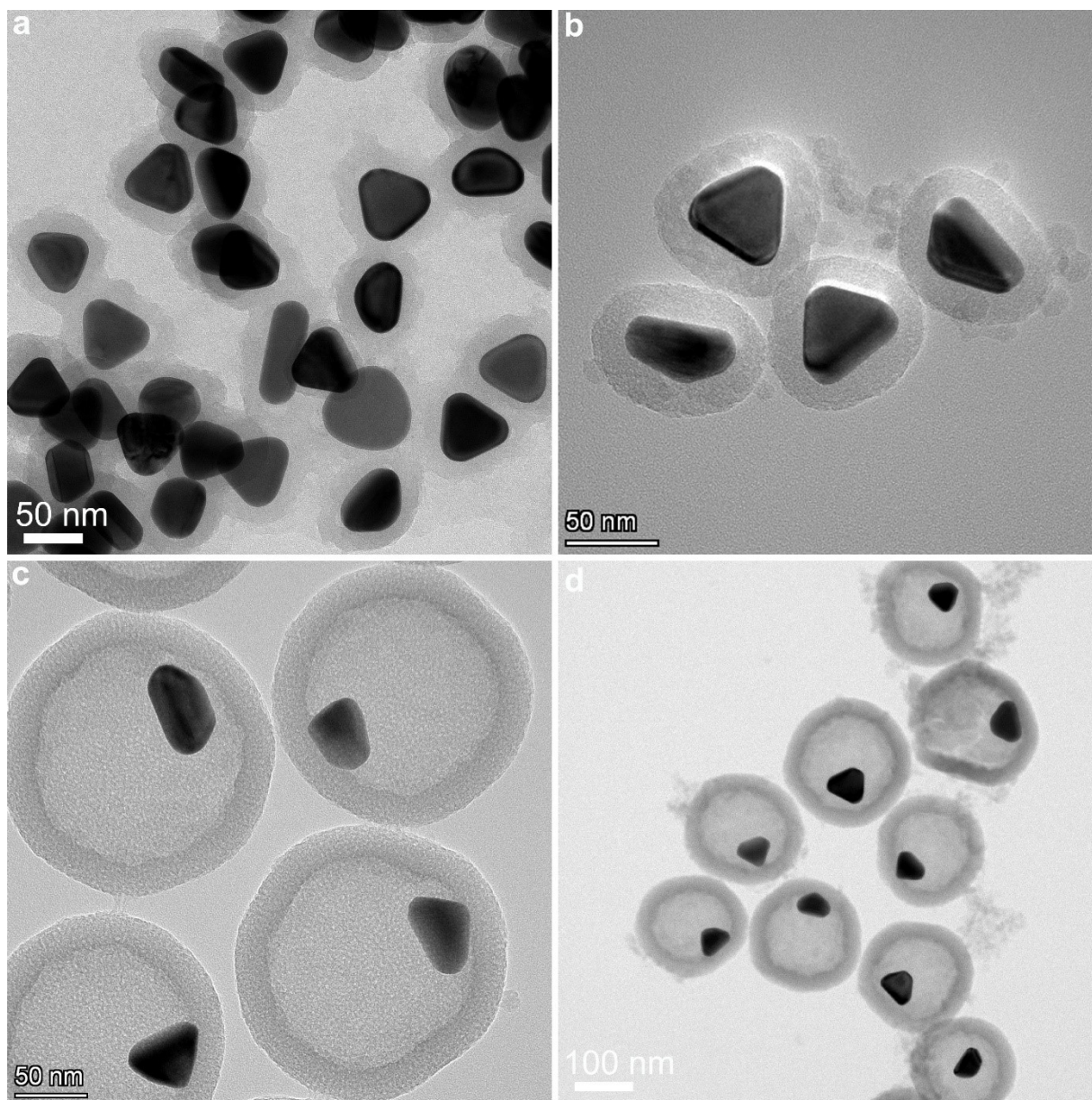


**Figure S17.** TEM images of (a) Au NT@mSiO<sub>2</sub> CS-10, (b) Au NT@mSiO<sub>2</sub> CS-20 after heating at 600 °C for one hour in an oven in ambient air, (c) Au NT@mSiO<sub>2</sub> YS-20, and (d) Au NT@mSiO<sub>2</sub> YS-30 after heating at 600 °C for one hour in an oven in ambient air (d).

## 9 Supporting Movie Information

Movie S1: LC-TEM movie showing the motion of Au NT@hollow-mSiO<sub>2</sub> yolk-shell nanoparticles recorded at a low electron dose rate of 215 e<sup>-</sup>/nm<sup>2</sup>/s. The movie is accelerated by a factor of 3 with respect to real time.

Movie S2: In-situ heating TEM movie showing the deformation and evaporation of a Au NT@mSiO<sub>2</sub> core-shell nanoparticle recorded at 1100 °C. The movie is accelerated by a factor of 3 with respect to real time.

## References:

1. Scarabelli, L.; Coronado-Puchau, M.; Giner-Casares, J. J.; Langer, J.; Liz-Marza'n, L. M., Monodisperse Gold Nanotriangles Size Control, Large-Scale Self-Assembly, and Performance in Surface-Enhanced Raman Scattering. *ACS Nano* **2014**, *8*, 5833-5842.
2. Xie, X.; van Huis, M. A.; van Blaaderen, A., Single-step coating of mesoporous SiO<sub>2</sub> onto nanoparticles: growth of yolk-shell structures from core-shell structures. *Nanoscale* **2021**, *13* (24), 10925-10932.
3. Johnson, P. B.; Christy, R. W., Optical Constants of the Noble Metals. *Physical Review B* **1972**, *6* (12), 4370-4379.
4. Fan, F.-R.; Liu, D.-Y.; Wu, Y.-F.; Duan, S.; Xie, Z.-X.; Jiang, Z.-Y.; Tian, Z.-Q., Epitaxial Growth of Heterogeneous Metal Nanocrystals: From Gold Nano-octahedra to Palladium and Silver Nanocubes. *J. Am. Chem. Soc.* **2008**, *130*, 6949–6951.
5. Bauer, E.; van der Merwe, J. H., Structure and growth of crystalline superlattices: From monolayer to superlattice. *Phys. Rev. B Condens Matter* **1986**, *33* (6), 3657-3671.
6. Xia, Y.; Xia, X.; Peng, H. C., Shape-Controlled Synthesis of Colloidal Metal Nanocrystals: Thermodynamic versus Kinetic Products. *J. Am. Chem. Soc.* **2015**, *137* (25), 7947-66.
7. Tran, R.; Xu, Z.; Radhakrishnan, B.; Winston, D.; Sun, W.; Persson, K. A.; Ong, S. P., Surface energies of elemental crystals. *Sci. Data.* **2016**, *3*.